Progress in Neuropsychopharmacology & Biological Psychiatry 140 (2025) 111422

Contents lists available at ScienceDirect

Progress in Neuropsychopharmacology & Biological Psychiatry

journal homepage: www.elsevier.com/locate/pnp

Long-lasting behavioral, molecular and functional connectivity alterations after chronic THC exposure during adolescence in mice

Laura Gómez-Acero [a,b], Federico Varriano [c], Nuria Sánchez-Fernández [a,b], Francisco Ciruela [a,b], Guadalupe Soria [c,d], Ester Aso [a,b,*]

[a] Pharmacology Unit, Department of Pathology and Experimental Therapeutics, School of Medicine and Health Sciences, Institute of Neurosciences, University of Barcelona, L'Hospitalet de Llobregat, Spain
[b] Neuropharmacology & Pain Group, Neuroscience Program, Bellvitge Institute for Biomedical Research, L'Hospitalet de Llobregat, Spain
[c] Brain Connectivity and Neuroimaging Group, School of Medicine and Health Sciences, Institute of Neurosciences, University of Barcelona, Barcelona, Spain
[d] CIBER de Bioingeniería, Biomateriales y Nanomedicina, Instituto de Salud Carlos III, Spain

ARTICLE INFO

Keywords:
Cannabis
Adolescence
Social interaction
Sensorimotor gating
Dopamine receptor
Adenosine receptor

ABSTRACT

Heavy and daily use of cannabis with high contents of Δ^9-tetrahydrocannabinol (THC) during adolescence is associated with an increased risk of developing psychotic disorders later in life. Here, we treated mice with THC during adolescence and found that this exposure impaired social interaction and increased vulnerability to develop sensorimotor gating deficiencies comparable to those previously described among heavy cannabis consumers. Importantly, we provide evidence on long-term cortico-striatal dysconnectivity induced by exposure to THC during adolescence and its correlation with impaired social interactions occurring later in adulthood. Moreover, we have observed long-lasting molecular alterations in key elements that regulate the mesolimbic dopaminergic system, namely on the balance between dopamine D_2, adenosine $A_{2A,}$ and cannabinoid CB_1 receptors in the striatum of treated mice. Together, these findings contribute to a better understanding of the neurobiological bases of the deleterious effects associated with cannabis abuse during adolescence.

1. Introduction

Cannabis consumption has increased worldwide in the last years, likely due to the decrease in risk perception derived from the legislative changes regulating medical and/or recreational use in many countries (Isorna et al., 2022). Epidemiological data reveal that heavy and daily use of cannabis with high content of the psychoactive compound Δ^9-tetrahydrocannabinol (THC) is associated with an increased risk of developing a cannabis use disorder (Budney and Borodovsky, 2017) and serious mental illness such as psychotic disorders (Di Forti et al., 2019). Importantly, male adolescents are particularly vulnerable to experiencing the neuropsychiatric symptoms associated with cannabis abuse, including both positive (*i.e.*, hallucinations and delusions) and negative (*i.e.*, cognitive and sociability deficits) symptoms of psychotic disorders, as well as anxiety and other mood disorders (Kiburi et al., 2021; Kozak et al., 2021; Leadbeater et al., 2019). To date, no specific therapies have been developed to treat these adverse effects associated with cannabis abuse despite the increasing demand for specialized treatment for problems related to cannabis consumption (European Monitoring Centre for Drugs and Drug Addiction, 2023). To progress toward more specific and effective therapies to deal with this growing health problem, it is essential to better understand the neurobiological bases of such deleterious effects of cannabis abuse. The main objective of this study is to contribute to this challenge by analyzing the long-lasting behavioral, molecular and functional connectivity alterations in the brain induced by chronic exposure to THC in male and female adolescent and adult mice.

Current knowledge of the neurobiological bases of psychotic disorders indicates that the dysregulation of dopaminergic brain circuits plays a fundamental role in the development of psychotic symptoms (McCutcheon et al., 2019). Specifically, psychotic symptoms such as hallucinations and delusions are related to the hyperactivity of the mesolimbic dopaminergic pathway and the increased activity of the dopamine (DA) D_2 receptor (D_2R) in the striatum (Seeman, 2013). However, current data from human imaging studies and preclinical reports point to a disruption in multiple afferent systems that regulate

* Corresponding author at: Pharmacology Unit, Department of Pathology and Experimental Therapeutics, School of Medicine and Health Sciences, University of Barcelona, C/Feixa Llarga s/n, 08907 L'Hospitalet de Llobregat, Spain.
E-mail address: ester.aso@ub.edu (E. Aso).

https://doi.org/10.1016/j.pnpbp.2025.111422
Received 24 February 2025; Received in revised form 2 June 2025; Accepted 8 June 2025
Available online 16 June 2025

dopaminergic neuron activity rather than to pathological changes within the DA system itself as the main alterations causing psychotic disorders (Grace and Gomes, 2019). In this sense, psychotic episodes induced by cannabis consumption with high THC content are concomitant with increased DA release in mesolimbic areas (Kuepper et al., 2010), which is mediated primarily by the THC-induced activation of CB_1R in the γ-aminobutyric acid (GABA)-ergic terminals projecting to dopaminergic neurons of the ventral tegmental area (VTA) (Bloomfield et al., 2016). Furthermore, increasing evidence suggests that altered dopaminergic signaling underlying psychotic symptoms could be associated with adenosine deficiency in certain brain regions (Boison et al., 2012). Different components of the adenosinergic system could contribute to the control of the mesolimbic dopaminergic system, but the strong antagonistic interaction between the adenosine A_{2A} receptor ($A_{2A}R$) and D_2R is known to play a key role (Ferré et al., 2018; Zhang et al., 2019). Thus, an imbalance between $A_{2A}R$ and D_2R has been observed in striatal samples from preclinical models of psychotic-like behaviors and patients with schizophrenia (Valle-León et al., 2021). Interestingly, $A_{2A}R$ also participates in the modulation of the THC effects on the dopaminergic system (Soria et al., 2004; Borgkvist et al., 2008; Justinová et al., 2011). Based on this evidence, the present study focusses first on the relationship between striatal levels of $A_{2A}R$, D_2R, and CB_1R as potential substrates underlying the harmful effects of chronic exposure to THC observed in adolescent and adult mice.

According to emerging theories holding that psychotic disorders result from the disruption of topological architecture in large-scale brain networks rather than from the lesion of isolated brain regions (Gao et al., 2023), we have also explored the potential alterations in the whole-brain connectome and cortico-striatal functional connectivity in THC-treated mice by using functional magnetic resonance imaging (fMRI) and graph theory as a powerful tool to accurately quantify the whole-brain connectivity network (Rubinov and Sporns, 2010) and its hypothetical correlation with aberrant behaviors later in adulthood.

Taken together, our findings contribute to a better understanding of the neurobiological bases of the long-lasting deleterious effects associated with cannabis abuse during adolescence.

2. Material and methods

2.1. Animals

Male and female C57BL/6 J mice aged 3 weeks (adolescents) and 4 months (adults) were purchased from Janvier Labs (Le Genest-Saint-Isle, France). Animals were housed 3–4 per cage and maintained under standard animal housing conditions in a 12-h dark-light cycle with free access to food and water. Mice were acclimated to animal facilities for 1 week and then they were randomly assigned to treatment groups. All the experiments were conducted under blind experimental conditions. Animal procedures were carried out following the guidelines of the European Communities Council Directive 2010/63/EU and with the approval of the local ethics committee of the University of Barcelona (417/18) and the Departament de Territori i Sostenibilitat from Generalitat de Catalunya (authorization number 10699).

2.2. Pharmacological treatment

THC was purchased from Sigma-Aldrich Inc. (St Louis, MO, USA) and dissolved in 5 % ethanol, 5 % Tween and 90 % saline for intraperitoneal (i.p.) injection. Mice received a daily THC (5 mg/kg) or vehicle i.p. administration for 1 month. The volume administered was 10 mL/kg of body weight. According to the formula for dose translation based on body surface area (Reagan-Shaw et al., 2008), the calculated human equivalent dose (HED) corresponds to 0.4 mg/kg of THC, which is approximately equivalent to the administration of 4 standard joint units (Casajuana Kögel et al., 2017) in a human being and resembles a heavy use of cannabis (Caulkins et al., 2020). Adolescent mice were treated with THC from post-natal day 28 (PND 28, early adolescence) to PND 60 (late adolescence). In the case of adult mice, they were treated with THC from PND 120 to PND 152.

2.3. Behavioral evaluation and sample collection

Behavioral testing started at PND 120 for the animals exposed to THC during adolescence and at PND 204 for those animals exposed to this drug during adulthood (Fig. 1A). Animals were consecutively evaluated in the elevated plus maze (EPM), the novel object recognition test (NORT), the three-chamber test, and the prepulse inhibition of the acoustic startle reflex test (PPI), as explained later. All behavioral tests were performed during the light phase with dim light conditions (100 lx maximum). Five days after the end of the PPI test, the animals were subjected to resting state functional magnetic resonance imaging (rs-fMRI). Two days after the rs-fMRI, the animals were sacrificed, and their brains samples were rapidly dissected, frozen, and stored at −80 °C until use. The striatum was dissected bilaterally using anatomical landmarks visible to the naked eye. Specifically, the region was identified based on its characteristic striated texture and its location beneath the cortex and adjacent to the lateral ventricles. All procedures were carried out by trained personnel familiar with the neuroanatomy of the mouse brain, ensuring consistency and reproducibility across samples.

2.3.1. Elevated plus maze (EPM)

Anxiety-like behavior was evaluated in the EPM, which consisted of a black plastic apparatus with four arms (15 × 5 cm) set in a cross from a neutral central square (5 × 5 cm) and elevated 40 cm above the floor. Two opposite arms were enclosed by vertical walls (closed arms), whereas the two other opposite arms had no protected edges (open arms). The total number of visits and the time spent in the open and closed arms were manually recorded through a closed-circuit camera system during the 5-min observation session.

2.3.2. Novel object recognition test (NORT)

Memory performance was assessed by NORT using a V-maze (da Cruz et al., 2020). Three hours after the end of the EPM test, the mice were placed within the V-maze (30 cm long x 5 cm wide each arm) and allowed to explore for 9 min two identical objects located at the ends of the maze arms. Each mouse's time exploring these objects was recorded through a closed-circuit camera system. Twenty-four hours later, the animals were reintroduced into the same V-maze for 9 min, but this time one of the familiar objects was replaced by a novel one. To assess memory performance, an object discrimination index (DI) was calculated using the following formula: $DI = (T_N - T_F)/(T_N + T_F)$, where T_N represents the time spent exploring the novel object, and T_F represents the time spent exploring the familiar object.

2.3.3. Three-chamber test

Social interaction and social memory of mice were evaluated in the three-chamber test one day after the end of NORT. The apparatus consists of a box (48 × 60 × 40 cm) divided into three chambers that are separated by two removable walls. First, the subject mouse was placed in the center of the middle chamber for 5 min as a habituation phase. Next, session 1 (sociability test) consisted of positioning a novel mouse (hereinafter referred to as mouse 1) inside a wire cage in one of the lateral chambers and a novel object (identical but empty wire cage) in the opposite one. The time spent exploring the novel mouse (mouse 1, T_M) or the novel object (T_O), was analyzed during 10 min. The social memory and novelty test (session 2) began immediately after the sociability test. In this test, the previous mouse (mouse 1) remained in its wire cage (now called the familiar mouse) and a novel mouse (mouse 2) was placed in the wire cage on the opposite side. Again, the time spent exploring the familiar mouse (mouse 1, T_F) or the novel mouse (mouse 2, T_N), was recorded manually for 10 min. Then, Sociability Index (SI) and Social Memory Index (SMI) were calculated, respectively, for the first

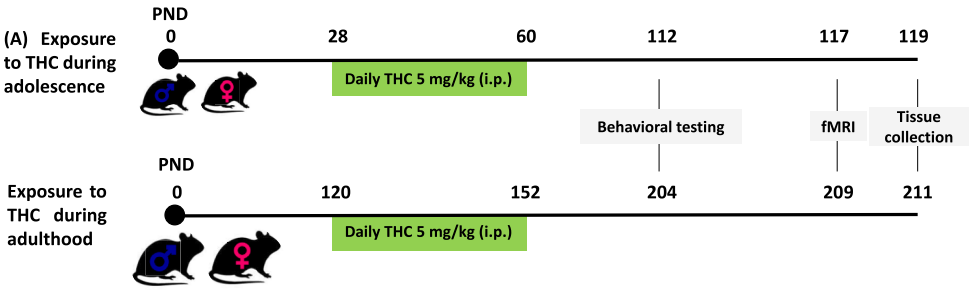

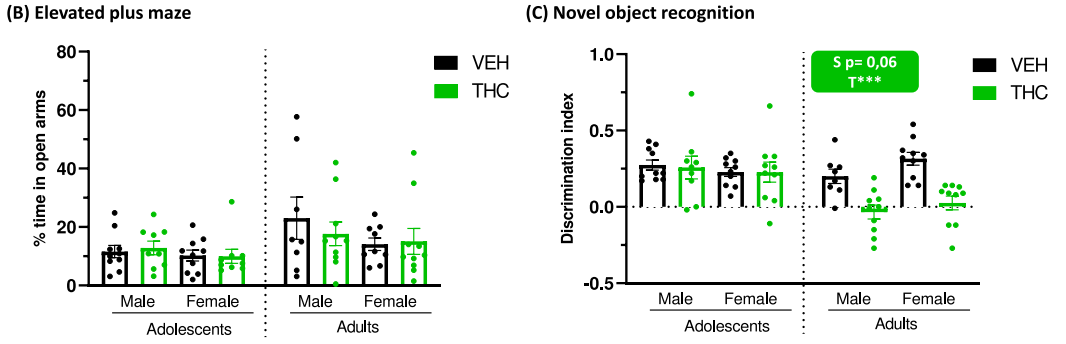

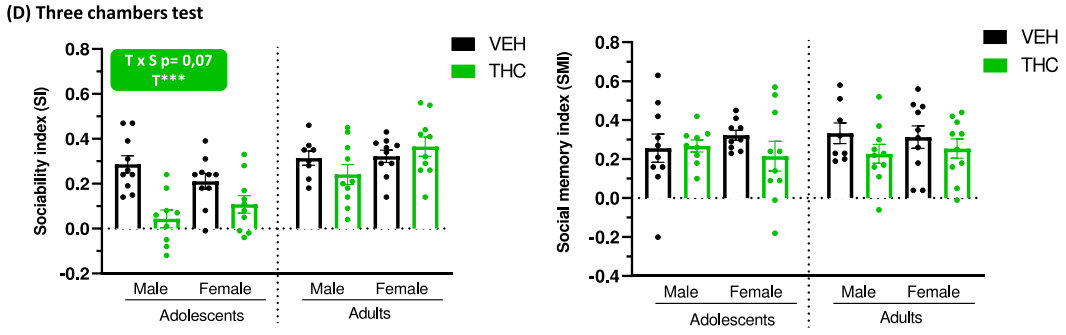

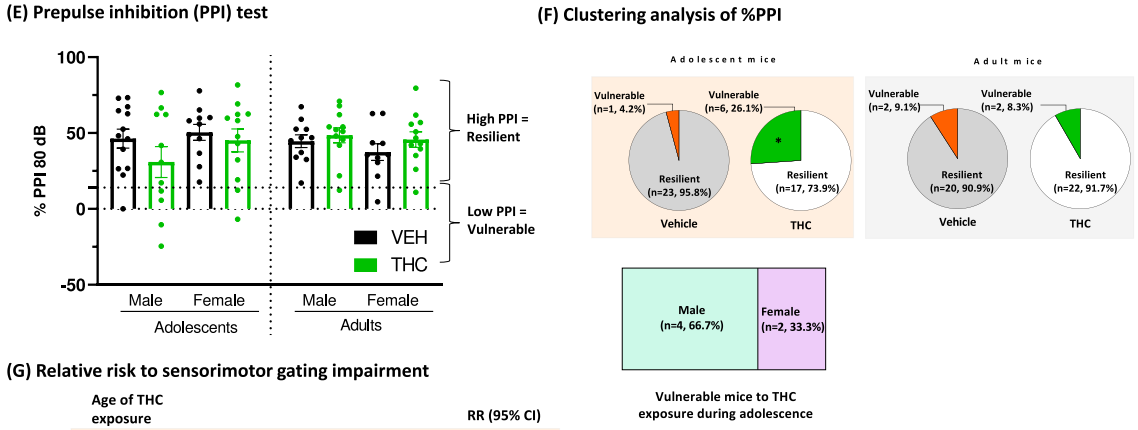

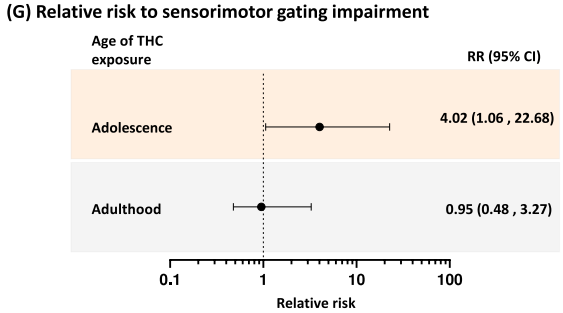

(caption on next page)

Fig. 1. **(A)** Schematic representation of the experimental design showing the treatment period with THC (5 mg/kg/day, i.p.) or vehicle (VEH) during adolescence (from PND 28 to PND 60) or adulthood (from PND 120 to PND 152) and the behavioral characterization of mice two months after the end of the chronic treatment. **(B)** Anxiety levels of treated mice were evaluated in the elevated plus maze (EPM). No significant changes in the time spent in open arms (%) were observed between the different experimental groups. **(C)** Memory performance of mice was evaluated in the novel object recognition test in a V-maze. A significant reduction in the discrimination index was observed in male and female mice treated with THC during adulthood. **(D)** Sociability (left) and social memory (right) indexes were assessed by the three-chamber test. Animals treated with THC during adolescence showed a significant sociability deficit later in life. No significant differences were observed in the social memory index between groups. **(E)** Sensorimotor gating was evaluated by the prepulse inhibition (PPI) of the acoustic startle test. Data show the percentage (%) of PPI response to a 120 dB acoustic stimulus preceded by an 80 dB prepulse. No significant differences between groups were observed in sensorimotor gating. Data are expressed as the mean ± SEM (n = 8–13/group). **(F)** Clustering analysis of % PPI 80 dB performed by the two-step cluster method identified two populations of mice, one vulnerable (low %PPI) and other resilient (high %PPI) to deficits in sensorimotor gating. A significantly higher proportion of the vulnerable population was found in mice exposed to THC during adolescence (χ^2, * $p < 0.05$). The vulnerable population has a higher amount of male than female. **(G)** An increased relative risk (RR) was observed when the age of exposure to THC was adolescence. T***: Treatment effect, $p < 0.001$; S: Sex effect; T x S: Treatment x sex interaction.

and second sessions: SI = (T_M-T_O)/(T_M + T_O); SMI = (T_N-T_F)/(T_N + T_F).

2.3.4. Prepulse inhibition of the acoustic startle reflex test (PPI)

Three hours after the end of the three-chamber test, the PPI was performed to evaluate sensorimotor gating in mice, which is known to be impaired under psychotic conditions (San-Martin et al., 2020). Two automated StartFear combined system chambers (LE116, Panlab, Harvard Instruments, Spain) were used to test PPI in mice, as previously described (Valle-León et al., 2021). Startle amplitude after prepulse (70, 75 and 80 dB) and pulse (120 dB) was automatically detected by PACKWIN V2.0 software. The percentage of prepulse inhibition (% PPI) for each prepulse intensity, was calculated as: %PPI = (startle amplitude on pulse alone – startle amplitude on prepulse trial)/(startle amplitude on pulse alone) x 100.

2.4. Resting-state functional magnetic resonance imaging (rs-fMRI)

2.4.1. Image acquisition

A 7.0 T BioSpec 70/30 horizontal animal scanner (Bruker BioSpin, Ettlingen, Germany), equipped with an actively covered gradient structure (400 mT/m, 12 cm inner diameter) was used to scan all mice. All the rs-fMRI acquisitions were performed during the light phase, approximately at the same time than the behavioral testing. Mice were placed in a Plexiglas holder and were fixed in a nose cone and exposed to a combination of anesthetic gases [medetomidine (bolus of 0.3 mg/kg, 0.6 mg/kg/h infusion) and isoflurane (0.5 %)]. This anesthetics combination is considered as an optimal protocol for preserving functional connectivity in rodent studies for its ability to minimize motion artifacts and stress while maintaining strong correspondence with functional connectivity patterns observed in awake animals (Grandjean et al., 2014; Paasonen et al., 2018). Thus, it has been recommended for standardizing fMRI acquisition and analysis procedures in rodents to enhance reproducibility (Mandino et al., 2020).

A 3D-localizer scan was used to ensure accurate position of the head at the isocenter of the magnet. T2-weighted image was obtained using a RARE sequence [effective TE = 33 ms, TR = 2.3 s, RARE factor = 8, voxel size = 0.08 × 0.08 mm^2, slice thickness = 0.5 mm]. The acquisition of rs-fMRI was performed using an echo planar imaging (EPI) sequence [TR = 2 s, TE = 19.4, voxel size 0.21 × 0.21 mm^2, slice thickness = 0.5 mm]; 420 volumes were acquired during 14 min.

2.4.2. rsfMRI: Image analysis and processing

Two approaches were used to evaluate functional connectivity, as previously described (Martínez-Torres et al., 2023; Conde-Berriozabal et al., 2023). On the one hand, whole brain connectivity was evaluated using global and regional network metrics (Rubinov and Sporns, 2010) and on the other hand a seed-based analysis was performed to evaluate connectivity of the nucleus accumbens (NAc) and Caudate Putamen (CPu) with the rest of the brain. For both approaches, rs-fMRI was preprocessed, including slice timing, motion correction by spatial realignment using SPM8, correction of EPI distortion by elastic registration to the T2-weighted volume using ANTs (Avants et al., 2008), detrend, smoothing with a full-width half maximum (FWHM) of 0.6 mm, frequency filtering of the time series between 0.01 and 0.1 Hz and regression by motion parameters. All these steps were performed using NiTime (http://nipy.org/nitime). Brain parcellation was performed by registration of a mouse brain atlas (Ma et al., 2008) to the T2-RARE acquisition of each subject using ANTs diffeomorphic registration. The region parcellation was then registered from the T2-weighted volume to the preprocessed mean rs-fMRI volume. The whole-brain functional brain network was estimated considering the grey matter regions obtained by parcellation as the network nodes. The connectivity between each pair of regions was estimated as the Fisher-z transform of the correlation between the average time series in each region. Network organization was quantified using regional and global graph metrics. Strength, local efficiency and clustering coefficient were calculated for every region, and the connectivity of the entire brain was quantified by the average strength, global and local efficiency, and the average clustering coefficient (Rubinov and Sporns, 2010). To perform the seed-based analysis, NAc and CPu were selected from the automatic parcellation. The average time series in the seed was computed and correlated with each voxel time series, resulting in a correlation map describing the connectivity of the striatum with the rest of the brain. The following regions of interest were identified from brain parcellation to evaluate their connectivity with the seed regions: (1) the cluster formed by the entorhinal (Ent), piriform (Pir), and insular cortex (Ins), (2) cingulate cortex (CgC), (3) hippocampus (Hipp), (4) medial prefrontal cortex (mPFC), (5) motor cortex, (6) sensory cortex, and parietal association cortex. Connectivity was quantified as the mean value of the correlation map in each region, considering only positive correlations.

2.5. Gel electrophoresis and immunoblotting

Striatal samples from mice selected randomly from all the treated mice of each experimental group were homogenized in ice-cold 10 mM Tris HCl (pH 7.4), 1 mM EDTA and 300 mM KCl buffer containing a protease inhibitor cocktail (Roche Molecular Systems, USA). The homogenates were centrifuged for 10 min at 1000 ×g. The resulting supernatants were centrifuged for 30 min at 12,000 ×g and the pellets were resuspended in 50 mM Tris HCl (pH 7.4) and 10 mM MgCl solution. Protein concentration was determined using the BCA protein assay kit (Thermo Fisher Scientific, Inc., Rockford, IL, USA) and equal amounts of protein (10 μg) for each sample were loaded and separated by electrophoresis on sodium dodecyl sulfate polyacrylamide gel electrophoresis (SDS-PAGE) (10 %) gels. Proteins were transferred to Hybond®-LFP polyvinylidene difluoride (PVDF) membranes (GE Healthcare, Chicago, IL, USA) using a Trans-Blot® SD semidry transfer cell (Bio-Rad, Hercules, CA, USA). Then, PVDF membranes were blocked with 5 % non-fat milk in phosphate buffered saline (PBS) buffer containing 0.05 % Tween-20 (PBS-T) for 45 min. After washing, membranes loaded with the striatal samples were incubated overnight at 4 °C with rabbit polyclonal anti-CB_1R (1:1500; Frontier Institute Co. Ltd., Shinko-nishi, Ishikari, Hokkaido, Japan), mouse monoclonal anti-$A_{2A}R$ (1:1000, Santa Cruz Biotechnology, Dallas, TX, USA, sc-32,261), rabbit polyclonal anti-

D_2R (1:1500; Frontier Institute Co. Ltd) and goat polyclonal anti-DAT (1:1000; Santa Cruz, sc-1433) antibodies in blocking solution overnight at 4 °C. Protein loading was monitored using an antibody against beta-tubulin (1:10000, Abcam, Cambridge, UK). PVDF membranes were washed with PBS-T three times (5 min each) before incubation with either a horseradish peroxidase (HRP)-conjugated goat antirabbit IgG (1/30000; Pierce Biotechnology, Rockford, IL, USA), HRP-conjugated rabbit anti-goat IgG (1/10000; Pierce Biotechnology) or HRP-conjugated goat anti-mouse (Thermo Fisher Scientific) in blocking solution at room temperature for 2 h. After washing the PVDF membranes with PBS-T 20 three times (5 min each), the immunoreactive bands were developed using a chemiluminescent detection kit (Thermo Fisher Scientific) and were detected with an Amersham Imager 600 (GE Healthcare Europe GmbH, Barcelona, Spain). Densitometric quantification was carried out with Image J (NIH, US). Bands were normalized to beta-tubulin.

2.6. Statistical analyses

Statistical analysis was performed with GraphPad Prism 9 (RRID: SCR_002798; San Diego, CA, USA). Statistical difference was set at $p < 0.05$. The number of samples/animals (n) in each group is indicated in the corresponding figure legend. Data normality was assessed using the Shapiro–Wilk test. Univariate outliers were assessed using the Grubbs's test, while multivariate outliers were detected by the Mahalanobis distance method. Comparisons between experimental groups were performed by two-way ANOVA with treatment and sex as between factors (behavioral test results, immunoblotting quantifications and fMRI results), followed by Tukey's *post hoc* when required. Pearson's correlation coefficients were calculated because all data were parametric. Correlations were statistically compared using the R Studio package cocor (Diedenhofen and Musch, 2015).

Clustering analyses were performed using IBM SPSS Statistics v24.0 software (Systat Software Inc., Chicago, IL, USA). Two-step cluster analysis was used to classify the entire cohort of animals according to their higher/lower %PPI 80 dB. Bayesian Criterion (BIC) was used to estimate of the maximum number of clusters, whereas the Euclidean method was used as a distance measure. To avoid bias in our data set, we did not predetermine the number of clusters. Chi-square analyses were performed to compare the percentage of mice in each cluster per treatment group. The effect size was calculated and expressed as the relative risk.

3. Results

3.1. Behavioral effects of chronic exposure to THC in adolescent and adult mice

Chronic THC treatment during adolescence or adulthood (Fig. 1A) did not produce any long-lasting alteration in the anxiety levels of male and female mice measured in the EPM (Fig. 1B). On the contrary, animals exposed to THC during adulthood, but not during adolescence, exhibited memory impairment in NORT later in life (Fig. 1C). Thus, two-way ANOVA revealed a significant effect of treatment ($F_{(1,34)} = 33.63$, $p < 0.0001$) in these animals characterized by a decrease in the discrimination index in both male and female animals chronically treated with THC during adulthood when compared to vehicle-treated mice.

Sociability and social memory deficits were evaluated in the three-chamber test. Two-way ANOVA revealed a treatment effect ($F_{(1,35)} = 20.32$, $p < 0.0001$) in animals exposed to THC during adolescence, but not during adulthood, and a tendency ($F_{(1, 35)} = 3.384$, $p = 0.07$) for the interaction between treatment and sex in the sociability index. Thus, animals chronically treated with THC during adolescence exhibited a reduced sociability index in adulthood, showing no greater interest in exploring a novel mouse than a novel inanimate object, a deficit that was more pronounced in male mice (Fig. 1D, left panel). No significant changes in social memory were observed in any of the experimental groups (Fig. 1D, right panel).

Impairments of PPI, a sensorimotor gating process, are observed in patients with schizophrenia (San-Martin et al., 2020) and in patients suffering cannabis-induced psychotic symptoms (Morales-Muñoz et al., 2014). In our experimental conditions, no significant PPI deficits were observed in any experimental group at any of the prepulse intensities evaluated, independently of the age when mice were exposed to THC or their sex (Fig. 1E shows representative results with 80 dB prepulse intensity). Similarly, no differences were observed between the groups in the startle response to any pulse intensity tested (data not shown). Statistical details of all the behavioral tests are included in Supplementary Table 1. However, clustering analysis identified two populations of mice, one vulnerable (low %PPI) and another resilient (high %PPI) to sensorimotor gating deficits. Interestingly, a significantly higher proportion of the vulnerable population was found only in mice exposed to THC during adolescence ($\chi^2_{(1)} = 4.452$, $p < 0.05$). Among these vulnerable mice treated with THC during adolescence, 67.7 % were males, revealing a sex-dependent predisposition to develop sensorimotor gating impairment in adolescent mice exposed to this drug (Fig. 1F). Estimating the relative risk of developing sensorimotor gating impairment revealed that mice exposed to THC during adolescence, but not during adulthood, were 4.02 times more likely to belong to the vulnerable group (low %PPI 80 dB) than those exposed to vehicle (Fig. 1G).

3.2. THC exposure during adolescence creates an imbalance between D_2R, CB_1R and $A_{2A}R$

Striatal dopamine dysfunction induced by THC is believed to be the basis for psychotic symptoms in cannabis users (Kuepper et al., 2010) and can be modulated by the adenosinergic system (Soria et al., 2004; Borgkvist et al., 2008; Justinová et al., 2011). Thus, we evaluated some key components of the dopaminergic, adenosinergic, and endocannabinoid systems in striatal samples of treated mice by immunoblotting (Fig. 2). Specifically, we determined the protein density of D_2R, $A_{2A}R$, CB_1R and the DA transporter (DAT). Two-way ANOVA revealed a significant effect of treatment in the levels of $A_{2A}R$ ($F_{(1,19)} = 7.17$, $p < 0.05$), CB_1R ($F_{(1,19)} = 6.23$, $p < 0.05$), and DAT ($F_{(1,17)} = 4.33$, $p = 0.05$) during adulthood, but not during adolescence, in mice (Fig. 2B). Statistical details of immunoblotting results are included in Supplementary Table 2.

As we hypothesized that an imbalance between these receptors could lead to psychotic-like alterations, we analyzed the correlations between their relative density. We observed a positive correlation between the density of D_2R and $A_{2A}R$, D_2R, and CB_1R, as well as $A_{2A}R$ and CB_1R in striatal samples in vehicle-treated animals regardless of age at the beginning of treatment (statistics are detailed in Fig. 2C). Interestingly, these correlations disappeared in mice that were treated with THC during adolescence, except the CB_1R and $A_{2A}R$ correlation that was preserved. Animals treated with THC during adulthood showed weaker correlations than those observed in vehicle-treated animals, but only the CB_1R-$A_{2A}R$ correlation was significantly lower ($p < 0.05$).

3.3. Long-term THC did not affect global brain network, but alters cortico-striatal connectivity in males exposed to THC during adolescence

Graph theory enables to quantify global network metrics and consequently to investigate the whole-brain network reorganization rather than isolated changes in the connectivity between specific brain areas[21] and facilitates the characterization of the connectivity between a specific region and the rest of the brain (Muñoz-Moreno et al., 2019). In this study, we use graph theory to explore the impact of exposure to THC during adolescence and adulthood on both global and regional functional network metrics, focusing on the NAc and CPu networks. Weighted and binary measures were calculated for both hemispheres.

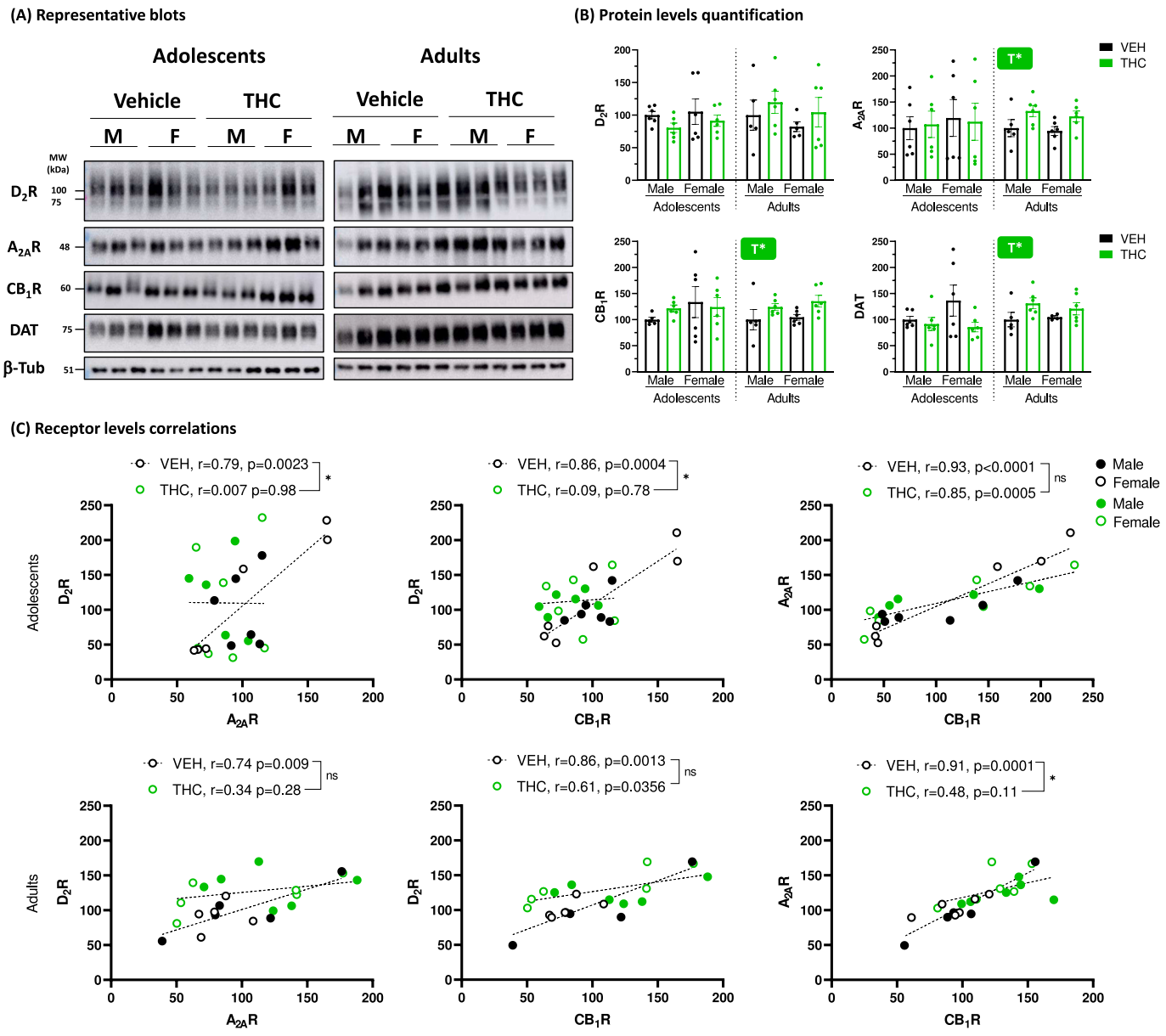

Fig. 2. Immunoblot detection of D_2R, CB_1R, $A_{2A}R$ and DAT in the striatum of male and female mice treated with THC or vehicle (VEH) during adolescence or adulthood. **(A)** Representative immunoblots showing the density of D_2R, CB_1R, $A_{2A}R$, DAT in striatal membrane fractions and corresponding β-tubulin loading control. Striatal membranes were analyzed by SDS-PAGE (10 μg of protein/lane) and immunoblotted using rabbit anti-D_2R, mouse anti-$A_{2A}R$, rabbit anti-CB_1R, goat anti-DAT and rabbit anti- β-tubulin antibodies (*see* Methods). **(B)** Relative quantification of D_2R, $A_{2A}R$, CB_1R, and DAT. The immunoblot protein bands corresponding to D_2R, $A_{2A}R$, CB_1R and DAT from male and female mice treated with THC or vehicle (VEH) during adolescence or adulthood (n = 5–6) were quantified by densitometric scanning. Values were normalized to the respective amount of β-tubulin in each lane to correct for protein loading. Results are expressed as percentage (mean ± SEM) and referred to VEH-treated male mice at each specific age. No significant effects were observed except for treatment in the expression of $A_{2A}R$, CB_1R and DAT in animals treated during adulthood. T*: Treatment effect, $p < 0.05$ **(C)** Bivariate correlations between D_2R, CB_1R and $A_{2A}R$ reveal a positive correlation between the expression of D_2R and $A_{2A}R$, D_2R and CB_1R, as well as $A_{2A}R$ and CB_1R in striatal samples in the VEH-treated animals independently of the age at the beginning of the treatment. That positive correlations disappeared in those mice that were treated with THC during adolescence, except the CB_1R and $A_{2A}R$ correlation, and were lower in animals treated with THC during adulthood compared to their corresponding VEH-treated control mice. * $p < 0.05$ comparison between treatment groups.

Regarding global brain networks, no statistically significant differences in global efficiency, local efficiency, clustering coefficient, or strength between groups were found after FDR correction (Table 1). Similarly, when we target NAc or CPu, no statistically significant differences in efficiency, clustering coefficient, or strength between groups were found after FDR correction (Table 1).

Next, we evaluated the changes in the functional connectivity between specific brain areas induced by chronic treatment with THC during adolescence or adulthood and the potential correlation with the observed behavioral alterations (Fig. 3). We performed a seed-based analysis of functional connectivity between NAc or CPu and selected brain regions previously described as involved in the development of psychotic-associated behaviors (Sabaroedin et al., 2023). Our results reveal alterations in the functional connectivity between left NAc and the left Enr, Pir, Ins cluster (treatment effect: $F_{(1,33)} = 10.67$, $p < 0.05$),), the left (sex effect: $F_{(1,33)} = 10.22$, $p < 0.05$) and right (treatment effect: $F_{(1,33)} = 8.87$, $p < 0.05$) cingulate cortex, left (treatment and sex interaction: $F_{(1,32)} = 9.12$, $p < 0.05$) and right (sex effect: $F_{(1,31)} = 10.73$,

Table 1
Functional network metrics of THC-treated mice during adolescence and adulthood.

	Mice exposed to THC during adolescence				Mice exposed to THC during adulthood			
	VEH male	VEH female	THC male	THC female	VEH male	VEH female	THC male	THC female
(A) Global network metrics								
Weigthed								
Global efficiency	0.099 ± 0.002	0.103 ± 0.002	0.100 ± 0.001	0.099 ± 0.001	0.104 ± 0.002	0.100 ± 0.002	0.102 ± 0.002	0.101 ± 0.002
Local efficiency	0.103 ± 0.002	0.105 ± 0.001	0.104 ± 0.001	0.104 ± 0.001	0.111 ± 0.002	0.108 ± 0.003	0.108 ± 0.002	0.104 ± 0.002
Clustering coefficient	0.094 ± 0.001	0.096 ± 0.001	0.095 ± 0.002	0.093 ± 0.001	0.096 ± 0.001	0.093 ± 0.001	0.095 ± 0.001	0.095 ± 0.002
Network strenght	10.350 ± 0.042	10.420 ± 0.037	10.370 ± 0.021	10.380 ± 0.023	10.470 ± 0.033	10.450 ± 0.066	10.450 ± 0.032	10.400 ± 0.042
Binary								
Global efficiency	0.770 ± 0.001	0.767 ± 0.003	0.767 ± 0.002	0.774 ± 0.002	0.766 ± 0.002	0.770 ± 0.002	0.771 ± 0.002	0.772 ± 0.002
Local efficiency	0.768 ± 0.002	0.766 ± 0.002	0.766 ± 0.002	0.771 ± 0.002	0.767 ± 0.002	0.769 ± 0.002	0.770 ± 0.002	0.769 ± 0.002
Clustering coefficient	0.585 ± 0.003	0.580 ± 0.005	0.581 ± 0.004	0.594 ± 0.004	0.583 ± 0.003	0.586 ± 0.004	0.587 ± 0.004	0.589 ± 0.004
Network degree	22.970 ± 0.124	22.800 ± 0.182	22.810 ± 0.153	23.180 ± 0.165	22.880 ± 0.162	23.090 ± 0.179	23.150 ± 0.151	23.040 ± 0.178
(B) Regional network metrics - Nucleus accumbens								
LEFT								
Weigthed								
Clustering coefficient	0.094 ± 0.004	0.096 ± 0.004	0.087 ± 0.003	0.089 ± 0.004	0.087 ± 0.004	0.095 ± 0.004	0.093 ± 0.006	0.090 ± 0.003
Network strenght	10.210 ± 0.112	10.350 ± 0.068	10.480 ± 0.035	10.500 ± 0.111	10.320 ± 0.063	10.450 ± 0.149	10.340 ± 0.107	10.420 ± 0.093
Efficiency	0.097 ± 0.004	0.103 ± 0.003	0.101 ± 0.005	0.099 ± 0.004	0.096 ± 0.004	0.103 ± 0.004	0.100 ± 0.006	0.097 ± 0.004
Binary								
Clustering coefficient	0.607 ± 0.010	0.584 ± 0.009	0.579 ± 0.005	0.579 ± 0.009	0.581 ± 0.008	0.590 ± 0.008	0.590 ± 0.012	0.590 ± 0.009
Network degree	22.560 ± 0.503	23.000 ± 0.799	23.890 ± 0.754	24.600 ± 0.733	23.880 ± 0.693	24.290 ± 0.522	23.100 ± 0.823	23.290 ± 0.808
Efficiency	0.780 ± 0.005	0.769 ± 0.005	0.767 ± 0.002	0.768 ± 0.004	0.768 ± 0.004	0.773 ± 0.004	0.772 ± 0.006	0.772 ± 0.005
(C) Regional network metrics - Caudate Putamen								
LEFT								
Weigthed								
Clustering coefficient	0.093 ± 0.0035	0.090 ± 0.003	0.094 ± 0.004	0.092 ± 0.003	0.108 ± 0.007	0.088 ± 0.004	0.102 ± 0.005	0.098 ± 0.004
Network strenght	9.995 ± 0.073	10.200 ± 0.068	10.140 ± 0.083	10.030 ± 0.054	10.190 ± 0.101	10.010 ± 0.031	10.080 ± 0.066	10.180 ± 0.110
Efficiency	0.093 ± 0.003	0.096 ± 0.002	0.098 ± 0.003	0.093 ± 0.002	0.108 ± 0.006	0.089 ± 0.002	0.101 ± 0.003	0.096 ± 0.002
Binary								
Clustering coefficient	0.603 ± 0.007	0.584 ± 0.012	0.598 ± 0.011	0.605 ± 0.011	0.580 ± 0.006	0.605 ± 0.013	0.604 ± 0.007	0.594 ± 0.014
Network degree	22.000 ± 0.667	23.220 ± 0.863	22.110 ± 0.484	21.670 ± 0.333	20.380 ± 0.944	22.630 ± 0.778	21.400 ± 0.921	21.860 ± 0.962
Efficiency	0.777 ± 0.003	0.764 ± 0.003	0.775 ± 0.005	0.779 ± 0.006	0.764 ± 0.004	0.779 ± 0.006	0.777 ± 0.004	0.773 ± 0.006

(A) Global network metrics of the functional connectomes. Global metrics of the weighted (A.1) and binary (A.2) functional connectome. (B) Regional network metrics of the functional connectomes. Functional regional network metrics of the weighted (B.1) and binary (B.2) functional connectome. No statistically significant differences between groups were found after FDR correction. Mean + SEM (n = 6–10 per group)

$p < 0.05$) mPFC in the animals treated with THC during adolescence (Fig. 3A and C), but not during the adulthood (Fig. 3B and D). Subsequent *post hoc* analyses revealed a lower connectivity between the left NAc and the left mPFC ($q < 0.05$) in male mice exposed to THC during adolescence compared to the vehicle control group. Moreover, a significant reduction in the functional connectivity between left NAc and the and left mPFC ($q < 0.01$) was found in female compared to male animals treated with vehicle during adolescence. No statistically significant differences were observed in functional connectivity between CPu and any region of interest in any case, despite a tendency to a reduction in functional connectivity of this seed area in animals treated during adolescence (Supplementary Fig. 1). Statistical details of this seed-based analysis of functional connectivity are included in Supplementary Tables 3 (treatment during adolescence) and 4 (treatment during adulthood).

Interestingly, the functional connectivity of the left CPu with the right CgC, the right Hipp, and the right mPFC, as well as the right CPu with the right and left CgC, the right and left Hipp, the right and left motor cortex, the left sensory cortex, and the parietal association were significantly correlated with the social interaction data ($q < 0.05$ in all cases), suggesting an anatomical substrate for the observed THC-induced alterations in social interaction in treated mice. Statistical details of the correlations between functional connectivity and behavior are included in Table 2.

4. Discussion

Exposure to THC during adolescence has been suggested to cause significant long-lasting changes in brain that are associated to an increased risk of developing psychotic symptoms. However, these THC-mediated plastic changes during this critical window for brain maturation are still poorly understood. This study provides compelling evidence of long-lasting, sex- and age-dependent behavioral, molecular, and brain functional connectivity alterations induced by chronic exposure to THC in mice. Specifically, daily exposure during adolescence (30 days) to a single dose of THC (5 mg/kg) induced sociability deficits and increased the risk of developing sensorimotor gating impairment during adulthood in male mice. It is relevant to note that this THC dose produces peaks in plasma concentrations in both adolescent and adult mice that are quantitatively comparable to those observed in adult nonmedical cannabis smokers (Torrens et al., 2020). Similarly, it is remarkable that those deleterious effects appear in the adulthood after a relatively

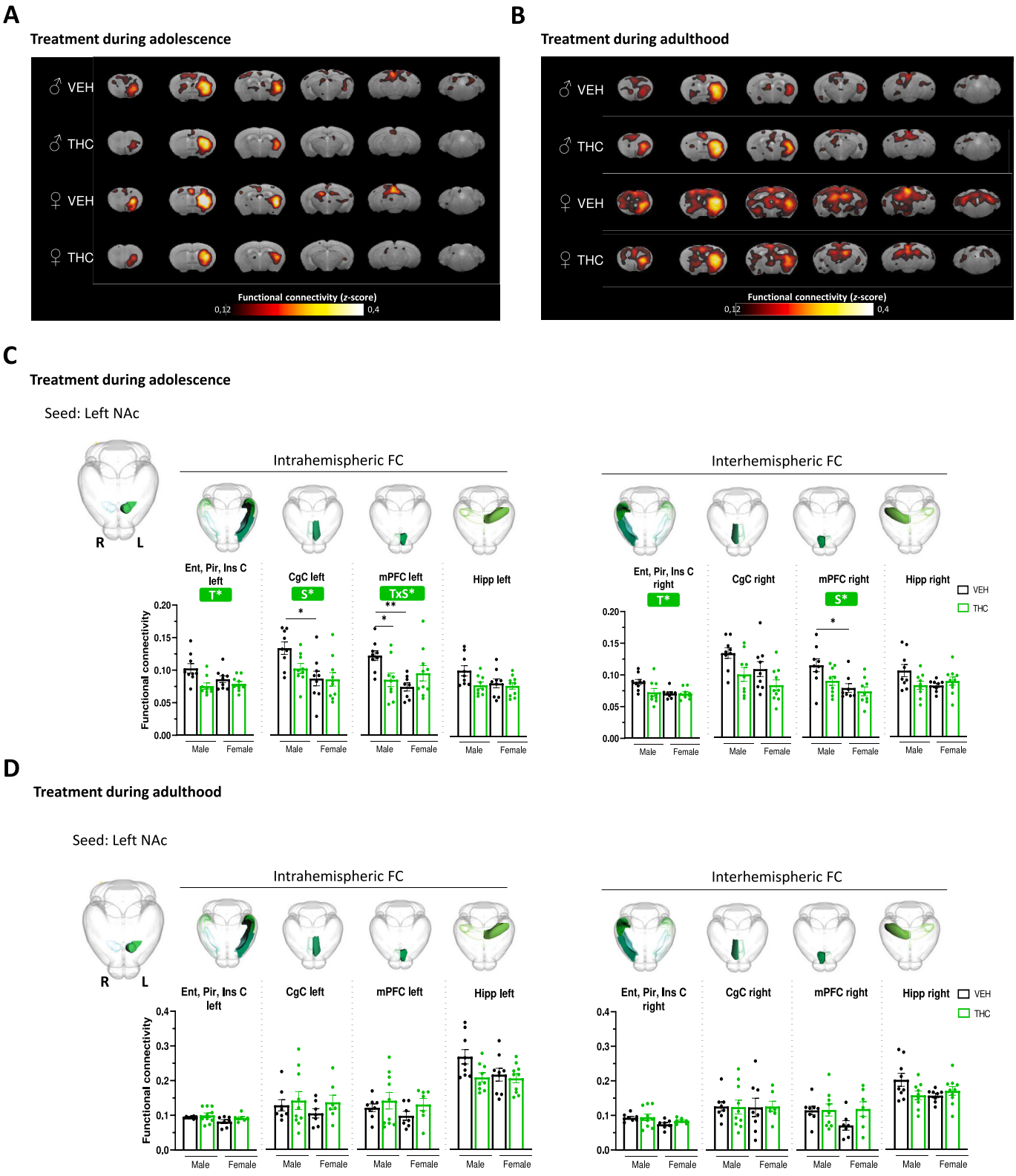

Fig. 3. (A-B) Average functional connectivity (FC) maps of left nucleus accumbens (NAc) in male and female mice exposed to THC or vehicle (VEH) during adolescence **(A)** and adulthood **(B)**. Color maps represent the average correlation value when >0.12. **(C—D)** Average functional connectivity of the left NAc with some of brain areas analyzed from the left hemisphere (intrahemispheric, left panels) and the right hemisphere (interhemispheric, right panels) are represented in mice exposed to THC or vehicle (VEH) during adolescence **(C)** and adulthood **(D)**. Each point represents data from an individual mouse. Data are mean ± SEM (n = 9–10/group). *q < 0.05, **q < 0.01 difference between indicated groups. CgC, cingulate cortex; Ent, entorhinal cortex; Hipp, hippocampus; mPFC, medial prefrontal cortex; Pir, piriform cortex. T*: Treatment effect, p < 0.05; S*: Sex effect, p < 0.05; T x S*: Treatment x Sex interaction, p < 0.05.

Table 2
Correlations between behavior and functional connectivity.

		%PPI	% Topen	NORT	SI	SMI			%PPI	% Topen	NORT	SI	SMI
Intrahemispheric							**Interhemispheric**						
Seed region							**Seed region**						
Caudate-putamen left							Caudate-putamen left						
Targeted areas							**Targeted areas**						
Entorhinal Piriform	*p-*						Entorhinal Piriform	p-					
Insular left	value	*N.S.*	*N.S.*	*N.S.*	**0.057**	*N.S.*	Insular right	value	*N.S.*	*N.S.*	*N.S.*	*N.S.*	*N.S.*
	r	0.128	0.033	−0.195	**0.378**	−0.122		r	0.100	0.103	−0.126	0.276	−0.109
	p-							p-				**p <**	
Cingulate left	value	*N.S.*	*N.S.*	*N.S.*	*N.S.*	*N.S.*	cingulate right	value	*N.S.*	*N.S.*	*N.S.*	**0.05**	*N.S.*
	r	0.028	0.123	−0.197	0.283	−0.039		r	0.123	0.092	−0.131	**0.405**	−0.129
	p-							p-				**p <**	
Hippocampus left	value	*N.S.*	*N.S.*	*N.S.*	*N.S.*	*N.S.*	hippocampus right	value	*N.S.*	*N.S.*	*N.S.*	**0.05**	*N.S.*
	r	0.048	0.046	0.034	0.220	−0.217		r	0.147	0.007	−0.197	**0.383**	−0.167
	p-							p-				**p <**	
mPFC left	value	*N.S.*	*N.S.*	*N.S.*	*N.S.*	*N.S.*	mPFC right	value	*N.S.*	*N.S.*	*N.S.*	**0.05**	*N.S.*
	r	−0.009	0.039	−0.212	0.196	0.004		r	0.034	0.138	−0.221	**0.371**	−0.096
	p-							p-					
Motor cortex left	value	*N.S.*	*N.S.*	*N.S.*	*N.S.*	*N.S.*	motor cortex right	value	*N.S.*	*N.S.*	*N.S.*	*N.S.*	*N.S.*
	r	0.037	0.108	−0.123	0.245	−0.061		r	0.066	0.155	−0.179	0.276	−0.073
Sensory cortex +							sensory cortex +						
parietal association	p-						parietal association	p-					
left	value	*N.S.*	*N.S.*	*N.S.*	*N.S.*	*N.S.*	right	value	*N.S.*	*N.S.*	*N.S.*	*N.S.*	*N.S.*
	r	0.043	0.017	−0.082	0.271	−0.223		r	0.162	−0.036	−0.016	0.205	−0.151
Seed region							**Seed region**						
Nucleus accumbens													
left							Nucleus accumbens left						
Targeted areas							**Targeted areas**						
Entorhinal Piriform	p-						Entorhinal Piriform	p-					
Insular left	value	*N.S.*	*N.S.*	*N.S.*	*N.S.*	*N.S.*	Insular right	value	*N.S.*	*N.S.*	*N.S.*	*N.S.*	*N.S.*
	r	0.169	0.038	−0.105	0.296	−0.019		r	0.118	0.052	−0.101	0.222	0.073
	p-							p-					
Cingulate left	value	*N.S.*	*N.S.*	*N.S.*	**0.069**	*N.S.*	cingulate right	value	*N.S.*	*N.S.*	*N.S.*	*N.S.*	*N.S.*
	r	0.022	0.064	−0.160	**0.372**	−0.008		r	0.093	−0.117	−0.074	0.314	−0.086
	p-							p-					
Hippocampus left	value	*N.S.*	*N.S.*	*N.S.*	*N.S.*	*N.S.*	hippocampus right	value	*N.S.*	*N.S.*	*N.S.*	*N.S.*	*N.S.*
	r	0.013	0.082	−0.194	0.268	−0.009		r	0.035	0.125	−0.080	0.253	0.141
	p-							p-					
mPFC left	value	*N.S.*	*N.S.*	*N.S.*	*N.S.*	*N.S.*	mPFC right	value	*N.S.*	*N.S.*	*N.S.*	*N.S.*	*N.S.*
	r	0.044	0.210	−0.279	0.277	0.037		r	0.068	−0.004	−0.272	0.238	0.011
	p-							p-					
Motor cortex left	value	*N.S.*	*N.S.*	*N.S.*	*N.S.*	*N.S.*	motor cortex right	value	*N.S.*	*N.S.*	*N.S.*	*N.S.*	*N.S.*
	r	0.005	0.115	−0.035	0.219	0.031		r	0.094	0.061	−0.053	0.197	−0.073
Sensory cortex +							sensory cortex +						
parietal association	p-						parietal association	p-					
left	value	*N.S.*	*N.S.*	*N.S.*	*N.S.*	*N.S.*	right	value	*N.S.*	*N.S.*	*N.S.*	*N.S.*	*N.S.*
	r	0.098	0.067	−0.021	0.214	0.031		r	0.204	−0.004	−0.168	0.075	0.058

short daily brain exposure to THC during the adolescence, since this compound has an elimination half-life ($t_{1/2}$) of 2 h in the mouse brain (Torrens et al., 2020). In addition, this chronic treatment with THC during the adolescence caused an imbalance between the striatal dopaminergic, cannabinoid, and adenosinergic systems later in adult mice. Importantly, exposure to THC during adolescence induced long-term cortico-striatal dysconnectivity, which was correlated with impaired social interactions occurring later in adulthood. Additionally, male and female mice chronically treated with THC during adulthood exhibited memory deficits later in life.

Interestingly, our results showing that chronic THC treatment during adolescence, but not during adulthood, reduced sociability in adulthood in male mice agree with some previous preclinical studies addressing this issue (Rubino and Parolaro, 2016; Renard et al., 2017), and mimic the sociability problems reported by chronic cannabis users (Blair et al., 2021). On the contrary, exposure to THC during adolescence in our experimental conditions did not influence memory performance later in life, despite previous findings associated exposure to adolescent THC with cognitive impairment in adult mice (Renard et al., 2014). However, this apparent discrepancy could be explained by the fact that we evaluated mice treated with THC during adolescence two months after the end of the treatment and previous reports demonstrated that cognitive impairment caused by a synthetic cannabinoid in adolescent rodents (Schneider and Koch, 2003) and THC in humans (Meier et al., 2012) can be reversed by sustained abstinence (Gorey et al., 2019; Tait et al., 2011). Interestingly, that long washout period was not enough to mitigate memory impairment in male and female mice treated with THC during adulthood. Although previous preclinical (Aso et al., 2015) and clinical studies (Mokrysz et al., 2016) suggested that chronic exposure to THC can also cause cognitive decline in adults, the present study is the first to report THC-induced memory alterations after such a prolonged period of abstinence in mice and warns about the detrimental chronic effects of recreational doses of THC during adulthood, which have been poorly investigated (Weinstein and Sznitman, 2020; Livne et al., 2023). Future research is planned to investigate the specific neurochemical and anatomical substrates underlying these cognitive impairments in mice chronically exposed to high doses of THC during adulthood.

Sensorimotor gating deficits measured by the PPI of the startle reflex are present in patients (San-Martin et al., 2020) and animal models (Van Den Buuse, 2010) of psychotic disorders including those related to

cannabis consumption (Morales-Muñoz et al., 2014), among other mental illnesses, and are considered to reflect alterations in the limbic-motor circuitry that regulates the capacity to properly filter out non-relevant sensory information from the external environment (Swerdlow et al., 2016). Our study reports that THC administration during adolescence did not induce global sensorimotor gating deficits in adult mice, in line with some previous studies (Llorente-Berzal et al., 2013; Poulia et al., 2021; Silva et al., 2016) but in contrast to some others (Renard et al., 2017; Abboussi et al., 2014; Abela et al., 2019). These contrasting findings could be explained by the fact that the PPI is very sensitive to a long list of variables, even within healthy populations (Swerdlow et al., 2016), so slightly different experimental conditions could lead to apparently opposing results. However, a clustering analysis of our results revealed that two significantly different populations can be identified among mice based on their PPI response (*i.e.* high PPI *vs* low PPI, or resilient *vs* vulnerable to sensorimotor gating deficits, respectively). Remarkedly, our data reveal a significantly higher proportion of the vulnerable population among mice exposed to THC during adolescence than during adulthood, which correlates with a higher relative risk of developing that sensorimotor gating impairment of mice exposed to THC during adolescence, but not during adulthood. Although the percentage of vulnerable mice was relatively low (≈26 %), our results align with epidemiological data showing that, even though only a small minority of cannabis users develop psychotic symptoms (Gage et al., 2016), there is a strong association between daily cannabis use during adolescence and increased rates of psychotic disorders (Di Forti et al., 2019). Multiple factors contribute to individual vulnerability to develop such psychotic symptoms, including patterns of cannabis use, exposure to childhood trauma, concurrent use of other drugs, genetic factors and, importantly, the age of onset of cannabis use, as well as sex (van der Steur et al., 2020; Kiburi et al., 2021). The greater vulnerability to the deleterious effects of THC in male mice suggested by our results, which resembles what occurs among cannabis users (Kiburi et al., 2021; Kozak et al., 2021; Leadbeater et al., 2019), could be related to the low circulating levels of estrogens in these animals. Indeed, these gonadal hormones are hypothesized to confer protection against psychotic symptoms and other neuropsychiatric signs associated with cannabis use (Prieto-Arenas et al., 2022).

Considering that psychotic symptoms in cannabis users have been associated with striatal dopamine dysfunction (Kuepper et al., 2010) and the already known role of the adenosinergic and endocannabinoid systems in the control of dopaminergic activity (Bloomfield et al., 2016; Boison et al., 2012), we next explored some key components of these neurotransmitter systems as potential substrates underlying the deleterious effects of chronic exposure to THC observed in mice. Our most remarkable finding is that, even though the total amount of each specific receptor is not altered in those adult mice treated with THC during the adolescence, a positive correlation between the levels of D_2R-$A_{2A}R$, D_2R-CB_1R exists in striatal samples from all experimental groups except in those mice that were treated with THC during adolescence, in which no significant correlations were identified except for levels of CB_1R and $A_{2A}R$. These results suggest that an accurate balance between D_2R and $A_{2A}R$/CB_1R expression could be instrumental in the precise regulation of striatal dopaminergic activity and that a perturbation of this equilibrium could underlie behavioral alterations. In this sense, previous findings revealed that deficiencies in the expression of D_2R (Lee et al., 2018), $A_{2A}R$ (López-Cruz et al., 2017) and CB_1R (Fyke et al., 2021), which are supposed to alter the balance between all three receptors, lead to altered sociability abilities in mice, as observed in adult mice exposed to THC during adolescence in the present study. Similarly, an imbalance between $A_{2A}R$ and D_2R has been observed in striatal samples from preclinical models exhibiting sensorimotor gating deficits and in patients with schizophrenia (Valle-León et al., 2021). These results point to the D_2R, $A_{2A}R$ and CB_1R equilibrium as a potential target to reverse or prevent the behavioral alterations induced by cannabis abuse.

To our knowledge, this is the first study conducted in mice that explores the long-term consequences of chronic exposure to THC in functional brain connectivity. Previous studies addressing the consequences of exposure to THC during adolescence reported short-term functional connectivity alterations, mainly in the hippocampal circuitry, but did not follow those animals until adulthood (Coleman et al., 2022). Our results revealed no differences between experimental groups in the global brain connectivity, but a significant cortico-striatal dysconnectivity in the adulthood induced by exposure to THC during adolescence. Similar functional connectivity deficits have previously been described in cannabis users (Mason et al., 2019) and patients with schizophrenia (Sabaroedin et al., 2023). Specifically, these alterations were found in the connectivity between the NAc and mPFC, and between the NAc and the Ent, Pir, Ins clusters in the left hemisphere. Interestingly, these deficits were limited to the limbic cortices, which are innervated by mesocortical DA (Berger et al., 1991). An equivalent dysconnectivity between the NAc and mPFC regions was previously reported in patients diagnosed with schizophrenia who used cannabis (Fischer et al., 2014; Thies et al., 2020). Notably, differences in functional connectivity between hemispheres were found, which could be related to the decreased number of fibers in the corpus callosum connecting both hemispheres previously reported to be associated with long-term cannabis use (Zalesky et al., 2012). Importantly, our data provide evidence of a significant correlation between social interaction data and functional connectivity between certain cortico-striatal regions and the hippocampus, suggesting that these circuitries could contribute to the THC-induced alterations in social interaction in mice exposed to this drug during the adolescence. Additional research is required to fully establish the relationship between the functional connectivity alterations and the behavioral and molecular alterations described here in adult mice chronically treated with THC during adolescence.

Overall, the present study provides novel insights into the neurochemical and neuroanatomical bases of the long-lasting deleterious effects associated with THC exposure during adolescence using a murine model that replicates some of the fundamental traits of the detrimental consequences of cannabis abuse. Our results support the hypothesis that chronic use of THC during adolescence can interfere with developmental processes occurring in the brain circuits critical for appropriate information processing in adulthood (Thies et al., 2020). Targeting such processes could be an optimal strategy to reduce the risk of developing neuropsychiatric disorders associated with adolescent cannabis exposure.

Supplementary data to this article can be found online at https://doi.org/10.1016/j.pnpbp.2025.111422.

Author contribution

LGA participated actively in the design of the study, performed all the experiments, analyzed the results and wrote the first draft of the manuscript. NSF contributed to the execution of the behavioral tests. GS and FV designed and processed the data of the fMRI experiments, interpreted the results and contributed to writing the manuscript. EA and FC conceived and designed the study, supervised the experiments and the analysis of the results and wrote the manuscript.

CRediT authorship contribution statement

Laura Gómez-Acero: Writing – original draft, Formal analysis, Data curation, Conceptualization. **Federico Varriano:** Writing – original draft, Formal analysis, Data curation. **Nuria Sánchez-Fernández:** Data curation. **Francisco Ciruela:** Writing – original draft, Funding acquisition, Formal analysis, Conceptualization. **Guadalupe Soria:** Writing – original draft, Supervision, Formal analysis, Data curation, Conceptualization. **Ester Aso:** Writing – review & editing, Writing – original draft, Supervision, Project administration, Funding acquisition, Formal analysis, Data curation, Conceptualization.

Ethical statement

The work has not been published before nor is being considered for publication in another journal.

All the authors have substantially contributed to the work and have read and approved the final version of the manuscript. None of the authors declare any conflict of interest. The authors are entirely responsible for the scientific content of the paper.

Animal procedures were conducted according to ethical ARRIVE guidelines and European Communities Council Directive 2010/63/EU, and approved by the local ethical committees of the University of Barcelona and Generalitat de Catalunya.

Funding sources

This study was supported by Plan Nacional sobre Drogas – Ministerio de Sanidad grants 2020I041 and 2024I054 to EA, and by Ministerio de Ciencia, Innovación y Universidades–Agencia Estatal de Investigación-FEDER funds/European Regional Development Fund – "a way to build Europe" grant PID2020-118511RB-I00 to FC. Founded by MCIN/AEI /10.13039/501100011033 "ESF Investing in your future", grant FPU19/03142 to LGA and grant PRE2019–088153 to NSF.

Declaration of competing interest

The authors declare that they have no known competing financial interests or personal relationships that could have appeared to influence the work reported in this paper.

Acknowledgments

We thank Centres de Recerca de Catalunya (CERCA) Programme/ Generalitat de Catalunya for IDIBELL institutional support and Maria de Maeztu MDM-2017-0729 and CEX2021-001159-M to Institut de Neurociències, Universitat de Barcelona. We are also grateful to the CannaLatan network members (CYTED-Programa Iberoamericano de Ciencia y Tecnología para el Desarrollo) for the fruitful discussion about the results. Moreover, we thank the staff of the Experimental 7 T magnetic resonance imaging (MRI) unit (IDIBAPS) for their technical support.

Data availability

Data will be made available on request.

References

Abboussi, O., Tazi, A., Paizanis, E., El Ganouni, S., 2014. Chronic exposure to WIN55,212-2 affects more potently spatial learning and memory in adolescents than in adult rats via a negative action on dorsal hippocampal neurogenesis. Pharmacol. Biochem. Behav. 120, 95–102.

Abela, A.R., Rahbarnia, A., Wood, S., Lê, A.D., Fletcher, P.J., 2019. Adolescent exposure to Δ9-tetrahydrocannabinol delays acquisition of paired-associates learning in adulthood. Psychopharmacology (Berl) 236, 1875–1886.

Aso, E., Sánchez-Pla, A., Vegas-Lozano, E., Maldonado, R., Ferrer, I., 2015. Cannabis-based medicine reduces multiple pathological processes in AβPP/PS1 mice. J. Alzheimers Dis. 43, 977–991.

Avants, B.B., Epstein, C.L., Grossman, M., Gee, J.C., 2008. Symmetric diffeomorphic image registration with cross-correlation: evaluating automated labeling of elderly and neurodegenerative brain. Med. Image Anal. 12, 26–41.

Berger, B., Gaspar, P., Verney, C., 1991. Dopaminergic innervation of the cerebral cortex: unexpected differences between rodents and primates. Trends Neurosci. 14, 21–27.

Blair, R.J.R., et al., 2021. Alcohol and Cannabis use disorder symptom severity, conduct disorder, and callous-unemotional traits and impairment in expression recognition. Front. Psych. 12, 714189.

Bloomfield, M.A.P., Ashok, A.H., Volkow, N.D., Howes, O.D., 2016. The effects of δ9-tetrahydrocannabinol on the dopamine system. Nature 539, 369–377.

Boison, D., Singer, P., Shen, H.Y., Feldon, J., Yee, B.K., 2012. Adenosine hypothesis of schizophrenia–opportunities for pharmacotherapy. Neuropharmacology 62, 1527–1543.

Borgkvist, A., Marcellino, D., Fuxe, K., Greengard, P., Fisone, G., 2008. Regulation of DARPP-32 phosphorylation by Δ^9-tetrahydrocannabinol. Neuropharmacology 54, 31–35.

Budney, A.J., Borodovsky, J.T., 2017. The potential impact of Cannabis legalization on the development of Cannabis use disorders. Prev Med (Baltim) 104, 31.

Casajuana Kögel, C., et al., 2017. The standard joint unit. Drug Alcohol Depend. 176, 109–116.

Caulkins, J.P., Pardo, B., Kilmer, B., 2020. Intensity of cannabis use: findings from three online surveys. Int. J. Drug Policy 79, 102740.

Coleman, J.R., et al., 2022. Changes in brain structure and function following chronic exposure to inhaled vaporised cannabis during periadolescence in female and male mice: a multimodal MRI study. Addict. Biol. 27, e13169.

Conde-Berriozabal, S., et al., 2023. M2 cortex circuitry and sensory-induced Behavioral alterations in Huntington's disease: role of superior colliculus. J. Neurosci. 43, 3379–3390.

da Cruz, J.F.O., et al., 2020. An alternative maze to assess novel object recognition in mice. Bio-Protoc. 10, 12 e3651.

Di Forti, M., et al., 2019. The contribution of cannabis use to variation in the incidence of psychotic disorder across Europe (EU-GEI): a multicentre case-control study. Lancet Psychiatry 6, 427–436.

Diedenhofen, B., Musch, J., 2015. Cocor: a comprehensive solution for the statistical comparison of correlations. PloS One 10, e0121945.

European Monitoring Centre for Drugs and Drug Addiction, 2023. European Drug Report 2023: Trends and Developments.

Ferré, S., et al., 2018. Essential control of the function of the Striatopallidal neuron by pre-coupled complexes of adenosine A2A-dopamine D2 receptor Heterotetramers and adenylyl cyclase. Front. Pharmacol. 9, 243.

Fischer, A.S., Whitfield-Gabrieli, S., Roth, R.M., Brunette, M.F., Green, A.I., 2014. Impaired functional connectivity of brain reward circuitry in patients with schizophrenia and cannabis use disorder: effects of cannabis and THC. Schizophr. Res. 158, 176–182.

Fyke, W., et al., 2021. Communication and social interaction in the cannabinoid-type 1 receptor null mouse: implications for autism spectrum disorder. Autism Res. 14, 1854–1872.

Gage, S.H., Hickman, M., Zammit, S., 2016. Association between Cannabis and psychosis: epidemiologic evidence. Biol. Psychiatry 79, 549–556.

Gao, Z., et al., 2023. The whole-brain connectome landscape in patients with schizophrenia: a systematic review and meta-analysis of graph theoretical characteristics. Neurosci. Biobehav. Rev. 148, 105144.

Gorey, C., Kuhns, L., Smaragdi, E., Kroon, E., Cousijn, J., 2019. Age-related differences in the impact of cannabis use on the brain and cognition: a systematic review. Eur. Arch. Psychiatry Clin. Neurosci. 269, 37–58.

Grace, A.A., Gomes, F.V., 2019. The circuitry of dopamine system regulation and its disruption in schizophrenia: insights into treatment and prevention. Schizophr. Bull. 45, 148–157.

Grandjean, J., Schroeter, A., Batata, I., Rudin, M., 2014. Optimization of anesthesia protocol for resting-state fMRI in mice based on differential effects of anesthetics on functional connectivity patterns. Neuroimage 102 (Pt 2), 838–847.

Isorna, M., Pascual, F., Aso, E., Arias, F., 2022. Impact of the legalisation of recreational cannabis use. Adicciones 20, 1694.

Justinová, Z., et al., 2011. Reinforcing and neurochemical effects of cannabinoid CB_1 receptor agonists, but not cocaine, are altered by an adenosine A_{2A} receptor antagonist. Addict. Biol. 16, 405–415.

Kiburi, S.K., Molebatsi, K., Ntlantsana, V., Lynskey, M.T., 2021. Cannabis use in adolescence and risk of psychosis: are there factors that moderate this relationship? A systematic review and meta-analysis. Subst. Abus. 42, 527–542.

Kozak, K., et al., 2021. A systematic review and meta-analysis of sex differences in cannabis use disorder amongst people with comorbid mental illness. Am. J. Drug Alcohol Abuse 47, 535–547.

Kuepper, R., et al., 2010. Does dopamine mediate the psychosis-inducing effects of cannabis? A review and integration of findings across disciplines. Schizophr. Res. 121, 107–117.

Leadbeater, B.J., Ames, M.E., Linden-Carmichael, A.N., 2019. Age-varying effects of cannabis use frequency and disorder on symptoms of psychosis, depression and anxiety in adolescents and adults. Addiction 114, 278–293.

Lee, Y., et al., 2018. Excessive D1 dopamine receptor activation in the dorsal striatum promotes autistic-like Behaviors. Mol. Neurobiol. 55, 5658–5671.

Livne, O., Potter, K.W., Schuster, R.M., Gilman, J.M., 2023. Longitudinal associations between Cannabis use and cognitive impairment in a clinical sample of middle-aged adults using Cannabis for medical symptoms. Cannabis Cannabinoid Res 9 (3), e933–e938.

Llorente-Berzal, A., et al., 2013. Sex-dependent psychoneuroendocrine effects of THC and MDMA in an animal model of adolescent drug consumption. PloS One 8, 11 e7838.

López-Cruz, L., et al., 2017. Adenosine A_{2A} receptor deletion affects social behaviors and anxiety in mice: involvement of anterior cingulate cortex and amygdala. Behav. Brain Res. 321, 8–17.

Ma, Y., et al., 2008. In vivo 3D digital atlas database of the adult C57BL/6J mouse brain by magnetic resonance microscopy. Front. Neuroanat. 2, 1.

Mandino, F., et al., 2020. Animal functional magnetic resonance imaging: trends and path toward standardization. Front. Neuroinform. 13, 78.

Martínez-Torres, S., et al., 2023. Peripheral CB_1 receptor blockade acts as a memory enhancer through a noradrenergic mechanism. Neuropsychopharmacology 48, 341–350.

Mason, N.L., et al., 2019. Cannabis induced increase in striatal glutamate associated with loss of functional corticostriatal connectivity. Eur. Neuropsychopharmacol. 29, 247–256.
McCutcheon, R.A., Abi-Dargham, A., Howes, O.D., 2019. Schizophrenia, dopamine and the striatum: from biology to symptoms. Trends Neurosci. 42, 205–220.
Meier, M.H., et al., 2012. Persistent cannabis users show neuropsychological decline from childhood to midlife. Proc. Natl. Acad. Sci. 109, 40.
Mokrysz, C., Freeman, T.P., Korkki, S., Griffiths, K., Curran, H.V., 2016. Are adolescents more vulnerable to the harmful effects of cannabis than adults? A placebo-controlled study in human males. Transl Psychiatry 6, 11 e961.
Morales-Muñoz, I., et al., 2014. Characterizing cannabis-induced psychosis: a study with prepulse inhibition of the startle reflex. Psychiatry Res. 220, 535–540.
Muñoz-Moreno, E., Tudela, R., López-Gil, X., Soria, G., 2019. Brain connectivity during Alzheimer's disease progression and its cognitive impact in a transgenic rat model. Network Neuroscience 4, 397–415.
Paasonen, J., Stenroos, P., Salo, R.A., Kiviniemi, V., Gröhn, O., 2018. Functional connectivity under six anesthesia protocols and the awake condition in rat brain. Neuroimage 172, 9–20.
Poulia, N., et al., 2021. Detrimental effects of adolescent escalating low-dose Δ9-tetrahydrocannabinol leads to a specific bio-behavioural profile in adult male rats. Br. J. Pharmacol. 178, 1722–1736.
Prieto-Arenas, L., Díaz, I., Carmen Arenas, M., 2022. Gender differences in dual diagnoses associated with Cannabis use: a review. Brain Sci. 12, 3 388.
Reagan-Shaw, S., Nihal, M., Ahmad, N., 2008. Dose translation from animal to human studies revisited. FASEB J. 22, 659–661.
Renard, J., Krebs, M.O., Le Pen, G., Jay, T.M., 2014. Long-term consequences of adolescent cannabinoid exposure in adult psychopathology. Front. Neurosci. 8, 361.
Renard, J., et al., 2017. Adolescent cannabinoid exposure induces a persistent sub-cortical hyper-dopaminergic state and associated molecular adaptations in the prefrontal cortex. Cereb. Cortex 27, 1297–1310.
Rubino, T., Parolaro, D., 2016. The impact of exposure to cannabinoids in adolescence: insights from animal models. Biol. Psychiatry 79, 578–585.
Rubinov, M., Sporns, O., 2010. Complex network measures of brain connectivity: uses and interpretations. Neuroimage 52, 1059–1069.
Sabaroedin, K., Tiego, J., Fornito, A., 2023. Circuit-based approaches to understanding Corticostriatothalamic dysfunction across the psychosis continuum. Biol. Psychiatry 93, 113–124.
San-Martin, R., et al., 2020. Meta-analysis of sensorimotor gating deficits in patients with schizophrenia evaluated by Prepulse inhibition test. Schizophr. Bull. 46, 1482–1497.
Schneider, M., Koch, M., 2003. Chronic pubertal, but not adult chronic cannabinoid treatment impairs sensorimotor gating, recognition memory, and the performance in a progressive ratio task in adult rats. Neuropsychopharmacology 28, 1760–1769.
Seeman, P., 2013. Schizophrenia and dopamine receptors. Eur. Neuropsychopharmacol. 23, 999–1009.
Silva, L., Black, R., Michaelides, M., Hurd, Y.L., Dow-Edwards, D., 2016. Sex and age specific effects of delta-9-tetrahydrocannabinol during the periadolescent period in the rat: the unique susceptibility of the prepubescent animal. Neurotoxicol. Teratol. 58, 88–100.
Soria, G., et al., 2004. Adenosine A_{2A} receptors are involved in physical dependence and place conditioning induced by THC. Eur. J. Neurosci. 20, 2203–2213.
Swerdlow, N.R., Braff, D.L., Geyer, M.A., 2016. Sensorimotor gating of the startle reflex: what we said 25 years ago, what has happened since then, and what comes next. J. Psychopharmacol. 30, 1072–1081.
Tait, R.J., Mackinnon, A., Christensen, H., 2011. Cannabis use and cognitive function: 8-year trajectory in a young adult cohort. Addiction 106, 2195–2203.
Thies, M.B., et al., 2020. Interaction of Cannabis use disorder and striatal connectivity in antipsychotic treatment response. Schizophr Bull Open 1, 1.
Torrens, A., et al., 2020. Comparative pharmacokinetics of Δ^9-tetrahydrocannabinol in adolescent and adult male mice. J. Pharmacol. Exp. Ther. 374, 151–160.
Valle-León, M., et al., 2021. Decreased striatal adenosine A_{2A}-dopamine D_2 receptor heteromerization in schizophrenia. Neuropsychopharmacology 46, 665–672.
Van Den Buuse, M., 2010. Modeling the positive symptoms of schizophrenia in genetically modified mice: pharmacology and methodology aspects. Schizophr. Bull. 36, 246–270.
van der Steur, S.J., Batalla, A., Bossong, M.G., 2020. Factors Moderating the Association Between Cannabis Use and Psychosis Risk: A Systematic Review. Brain Sci. 10, 97–114.
Weinstein, G., Sznitman, S.R., 2020. The implications of late-life cannabis use on brain health: a mapping review and implications for future research. Ageing Res. Rev. 59, 101041.
Zalesky, A., et al., 2012. Effect of long-term cannabis use on axonal fibre connectivity. Brain 135, 2245–2255.
Zhang, X., et al., 2019. Balance between dopamine and adenosine signals regulates the PKA/Rap1 pathway in striatal medium spiny neurons. Neurochem. Int. 122, 8–18.